Anal. Chem. **2010,** *82,* 1245–1252

DNA Interaction with Palladium Chelates of Biogenic Polyamines Using Atomic Force Microscopy and Voltammetric Characterization

O. Corduneanu,[†] A.-M. Chiorcea-Paquim,[†] V. Diculescu,[†] S. M. Fiuza,[‡] M. P. M. Marques,[‡] and A. M. Oliveira-Brett*,[†]

Departamento de Química, and Unidade I&D "Química-Física Molecular" and Departamento de Bioquímica, Faculdade de Ciências e Tecnologia, Universidade de Coimbra, Portugal

The interaction of double-stranded DNA with two polynuclear Pd(II) chelates with the biogenic polyamines spermidine (Spd) and spermine (Spm), Pd(II)−Spd and Pd(II)−Spm, as well as with the free ligands Spd and Spm, was studied using atomic force microscopy (AFM) at a highly oriented pyrolytic graphite (HOPG) surface, voltammetry at a glassy carbon (GC) electrode, and gel electrophoresis. The AFM and voltammetric results showed that the interaction of Spd and Spm with DNA occurred even for a low concentration of polyamines and caused no oxidative damage to DNA. The Pd(II)−Spd and Pd(II)−Spm complexes were found to induce greater morphological changes in the dsDNA conformation, when compared with their ligands. The interaction was specific, inducing distortion and local denaturation of the B-DNA structure with release of some guanine bases. The DNA strands partially opened give rise to palladium intra- and interstrand cross-links, leading to the formation of DNA adducts and aggregates, particularly in the case of the Pd(II)−Spd complex.

The development of new chemotherapeutic agents led to the synthesis of polynuclear metal complexes, a new class of third generation anticancer agents with specific chemical and biological properties designed as alternatives to first-generation agents such as cisplatin (*cis*-dichlorodiammineplatinum(II), *cis*-$Pt(Cl_2(NH_3)_2)$.[1−18] Many of these complexes were found to yield DNA adducts through long-distance intra- and interstrand cross-links, not available to the mononuclear platinum compounds previously known,[9,12−18] suggesting the possibility of escaping the conventional mechanism of cisplatin resistance related to the DNA damage recognition and repair. Furthermore, it is known that a simple chemical modification in the drug may alter its DNA binding properties, since it can lead to significant conformational changes, thus ruling its cytotoxic activity. This enables the functionalization of DNA-binding modes, in order to obtain compounds displaying not only selective but also enhanced and unique anticancer properties.

The biogenic polyamines spermidine (Spd, $H_2N(CH_2)_3NH(CH_2)_4NH_2$) and spermine (Spm, $H_2N(CH_2)_3NH(CH_2)_4NH(CH_2)_3NH_2$), Scheme 1, were recently addressed in several studies of polynuclear metal complexes as potential antineoplastic drugs,[1−3,5−10] due to their important biological activity and affinity for DNA. Their role in the proliferation and differentiation of cells coupled to the presence of cationic groups located at regular intervals within the molecule enable a selective interaction with the electronegative groups of DNA. In vitro they act as compaction agents and provide a means for the purification of nucleic acids,

* To whom correspondence should be addressed. Address: Departamento de Química, Faculdade de Ciências e Tecnologia, Universidade de Coimbra, 3004-535 Coimbra, Portugal. E-mail: brett@ci.uc.pt.

[†] Departamento de Química.

[‡] Unidade I&D "Química-Física Molecular" and Departamento de Bioquímica.

(1) Navarro-Ranninger, C.; Zamora, F.; López-Solera, I.; Masaguer, J. R.; Pérez, J. M.; Alonso, C.; Martínez-Carrera, S. *J. Inorg. Biochem.* **1992**, *46*, 267–279.

(2) Navarro-Ranninger, C.; Zamora, F.; Masaguer, J. R.; Pérez, J. M.; González, V. M.; Alonso, C. *J. Inorg. Biochem.* **1993**, *52*, 37–49.

(3) Navarro-Ranninger, C.; Amo Ochoa, P.; Masaguer, J. R.; Pérez, J. M.; González, V. M.; Alonso, C. *J. Inorg. Biochem.* **1994**, *53*, 177–190.

(4) Codina, G.; Caubet, A.; López, C.; Moreno, V.; Molins, E. *Helv. Chim. Acta* **1999**, *82*, 1025–1037.

(5) Farrell, N. In *Metal ions in biological systems*; Sigel, H., Ed.; Marcel Dekker Inc.: New York, 1996; Vol. 42, pp 251−296.

(6) Marques, M. P. M.; Girão, T.; Pedroso De Lima, M. C.; Gameiro, A.; Pereira, E.; Garcia, P. *BBA−Mol. Cell. Res.* **2002**, *1589*, 63–70.

(7) Teixeira, L. J.; Seabra, M.; Reis, E.; Girão da Cruz, M. T.; Pedroso de Lima, M. C.; Pereira, E.; Miranda, M. A.; Marques, M. P. M. *J. Med. Chem.* **2004**, *47*, 2917–2925.

(8) Fiuza, S. M.; Amado, A. M.; Oliveira, P. J.; Sardão, V. A.; Batista de Carvalho, L. A. E.; Marques, M. P. M. *Lett. Drug Des. Discovery* **2006**, *3*, 149–151.

(9) Soares, A. S.; Fiúza, S. M.; Gonçalves, M. J.; Batista de Carvalho, L. A. E.; Marques, M. P. M.; Urbano, A. M. *Lett Drug Des. Discovery* **2007**, *4*, 460–463.

(10) Moriarity, B.; Nováková, O.; Farrell, N.; Brabec, V.; Kašpárková, J. *Arch. Biochem. Biophys.* **2007**, *459*, 264–272.

(11) Gebel, T.; Lantzsch, H.; Plessow, K.; Dunkelberg, H. *Mutat. Res.−Gen. Tox. En.* **1997**, *389*, 183–190.

(12) Hubbard, R. D.; Fidanze, S. *Compr. Med. Chem. II* **2007**, *7*, 129–148.

(13) Aebi, S.; Kurdi-Haidar, B.; Gordon, R.; Cenni, B.; Zheng, H.; Fink, D.; Christen, R. D.; Boland, C. R.; Koi, M.; Fishel, R.; Howell, S. B. *Cancer Res.* **1996**, *56*, 3087–3090.

(14) Perego, P.; Caserini, C.; Gatti, L.; Carenini, N.; Romanelli, S.; Supino, R.; Colangelo, D.; Viano, I.; Leone, R.; Spinelli, S.; Pezzoni, G.; Manzotti, C.; Farrell, N.; Zunino, F. *Mol. Pharmacol.* **1999**, *55*, 528–534.

(15) Abu-Surrah, A. S.; Al-Sadoni, H. H.; Abdalla, M. Y. *Cancer Ther.* **2008**, *6*, 1–10.

(16) Abu-Surrah, A. S.; Kettunen, M.; Lappalainen, K.; Piironen, U.; Klinga, M.; Leskelä, M. *Polyhedron* **2002**, *21*, 27–31.

(17) Manzotti, C.; Pratesi, G.; Menta, E.; Di Domenico, R.; Cavalletti, E.; Fiebig, H. H.; Kelland, L. R.; Farrell, N.; Polizzi, D.; Supino, R.; Pezzoni, G.; Zunino, F. *Clin. Cancer Res.* **2000**, *6*, 2626–2634.

(18) Wheate, N. J.; Collins, J. G. *Curr. Med. Chem.-Anticancer Agents* **2005**, *5*, 267–279.

10.1021/ac902127d
Published on Web 01/20/2010

Scheme 1. Representation of the Most Stable Structures of Spermidine and Spermine, in Their N-Protonated Form (Physiological Species)

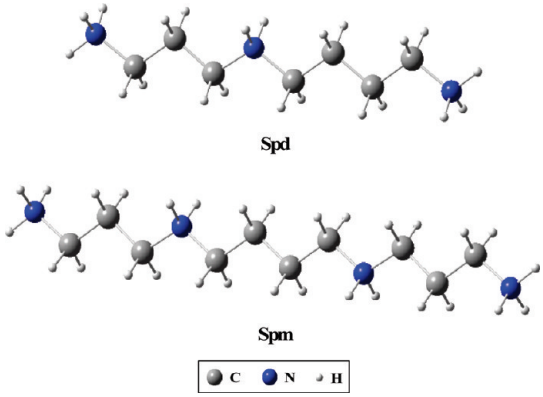

thus being used for the selective precipitation of DNA.[19,20] In vivo, in turn, they act as agents of compaction for the packing of the genomic DNA in sperm[21] and may have a similar function in the delivery of pharmaceutical drugs to DNA.[22] The potential importance of these polydentate ligands in polynuclear metal chelates was first suggested through an in vitro study,[1] when a Pd(II) complex with Spd was found to display a higher antiproliferative activity toward cancer cells than cisplatin. Lately, several cationic polynuclear Pd(II) chelates comprising two or three cisplatin-like moieties linked by variable length aliphatic polyamines have been assessed, and their antiproliferative and cytotoxic effect toward several human cancer cell lines was demonstrated,[6−9] with their activity being related to their conformational preferences at physiological conditions.[23,24] Understanding the mechanisms of action of these metal-based agents at a molecular level and their interaction with nucleic acids is essential for the establishment of structure−activity relationships (SAR's) that will enable the design of new and improved anticancer drugs.

The present paper is a report of an atomic force microscopy (AFM) and differential pulse (DP) voltammetric study of the interaction established with double-stranded DNA (dsDNA) by two polynuclear palladium chelates with Spd and Spm as polydentate ligands. Pd(II)−Spd is a trinuclear 2,2,2/c,c,c Pd(II) chelate of general formula $(PdCl_2)_3(Spd)_2$, comprising two Spd units as bridging ligands. Pd(II)−Spm is a dinuclear 2,2/c,c chelate of general formula $(PdCl_2)_2Spm$ that contains one tetraamine ligand (Spm) acting as a linker for both metal centers and yields two identical six-membered intramolecular rings in a trans orientation relative to each other.

The mechanism of interaction of Pd(II)−Spd and Pd(II)−Spm with dsDNA was established on the basis of the correlations between the DNA redox behavior at a glassy carbon (GC) electrode and the DNA conformational modifications observed onto a highly oriented pyrolytic graphite (HOPG) surface, obtained before and after the dsDNA interaction with both complexes, Pd(II)−Spd and Pd(II)−Spm, and the ligands, Spd and Spm. Nondenaturing agarose gel (0.5%) electrophoretic experiments were also performed in order to evaluate the morphological modifications obtained before and after dsDNA interaction with the Pd(II) polyamine complexes.

(19) Hoopes, B. C.; McClure, W. R. *Nucleic Acids Res.* **1981**, *9*, 5493–5504.
(20) Murphy, J. C.; Wibbenmeyer, J. A.; Fox, G. E.; Willson, R. C. *Nat. Biotechnol.* **1999**, *17*, 822–823.
(21) Bednar, J.; Furrer, P.; Stasiak, A.; Dubochet, J.; Egelman, E. H.; Bates, A. D. *J. Mol. Biol.* **1994**, *235*, 825–847.
(22) Rolland, A. P. *Crit. Rev. Ther. Drug Carrier Syst.* **1998**, *15*, 143–198.
(23) Amado, A. M.; Fiuza, S. M.; Marques, M. P. M.; Batista de Carvalho, L. A. E. *J. Chem. Phys.* **2007**, *127*, 185104–185113.
(24) Fiuza, S. M.; Amado, A. M.; Marques, M. P. M.; Batista de Carvalho, L. A. E. *J. Phys. Chem. A* **2008**, *112*, 3253–3259.

EXPERIMENTAL SECTION

Materials and Reagents. Spermidine and spermine were purchased from Sigma-Aldrich and kept at 4°C. Solutions of either Spm or Spd were freshly prepared before each experiment by dilution of the appropriate quantity in the supporting electrolyte. Calf thymus dsDNA and all the other reagents were Merck analytical grade. A stock solution of 300 μg mL^{-1} dsDNA was prepared in deionized water and kept at 4 °C. The solutions were diluted to the desired concentration by mixing buffer supporting electrolyte. The supporting electrolyte solutions used were pH 4.5, 0.1 M acetate buffer and pH 7.0, 0.1 M phosphate buffer. Pd−spermidine (Pd(II)−Spd or $(PdCl_2)_3(Spd)_2$) and Pd−spermine (Pd(II)−Spm or $(PdCl_2)_2Spm$) were synthesized in the Research Unit "Molecular Physical-Chemistry", Coimbra, Portugal, according to published procedures,[3,4] with slight modifications. Solutions of either Pd(II)−Spd or Pd(II)−Spm were freshly prepared before each experiment by dilution of the appropriate quantity in pH 7.0, 0.1 M phosphate buffer. All solutions were prepared using analytical grade reagents and purified water from a Millipore Milli-Q system (conductivity $\leq$0.1 μS cm^{-1}).

Nitrogen saturated solutions were obtained by bubbling high purity N_2 for a minimum of 10 min through the solution, and a continuous flow of pure gas was maintained over the solution during the voltammetric experiments.

Microvolumes were measured using EP-10 and EP-100 plus motorized microliter pippettes (Rainin Instrument Co. Inc., Woburn, USA). The pH measurements were carried out with a Crison micropH 2001 pH meter with an Ingold combined glass electrode. All experiments were carried out at room temperature (25 ± 1 °C).

Atomic Force Microscopy. HOPG, grade ZYB of 15 × 15 × 2 mm^3 dimensions, from Advanced Ceramics Co., USA, was used as a substrate in the AFM study. The HOPG was freshly cleaved with adhesive tape prior to each experiment and imaged by AFM in order to establish its cleanliness.

AFM was performed in the magnetic AC mode (MAC Mode) AFM, with a PicoScan controller from Agilent Technologies, Tempe, AZ, USA. All the AFM experiments were performed with a CS AFM S scanner with a scan range of 6 μm in $x-y$ and 2 μm in z, from Agilent Technologies. Silicon type II MAClevers of 225 μm length, 2.8 N m^{-1} spring constants, and 60−90 kHz resonant frequencies in air (Agilent Technologies) were used. All AFM images were topographical and were taken with 256 samples/line × 256 lines and scan rates of 0.8−2.0 lines s^{-1}. When necessary, MAC mode AFM images were processed by flattening in order to remove the background slope and the contrast and brightness were adjusted. Section analyses were performed with PicoScan software version 5.3.3, Agilent Technologies, and with Origin version 6.0, Microcal Software, Inc., USA.

Voltammetric Parameters and Electrochemical Cells. The voltammetric experiments were performed using an Autolab

running with GPES 4.9 software, Eco-Chemie, Utrecht, The Netherlands. The DP voltammetry conditions were as follows: pulse amplitude, 50 mV; pulse width, 70 ms; step potential, 2 mV; scan rate, 5 mV s^{-1}. Measurements were carried out in a 0.5 mL one-compartment electrochemical cell using a GC electrode (d = 1.5 mm), with a Pt wire counter electrode and an Ag/AgCl (3 M KCl) electrode as reference.

DNA Gel Electrophoresis. For the preparation of control dsDNA solutions for DNA gel electrophoresis, 50 μg mL^{-1} or 100 μg mL^{-1} dsDNA in pH 7.0, 0.1 M phosphate buffer was used, stored at room temperature during 24 h. For the preparation of DNA−Pd(II)−Spd and DNA−Pd(II)−Spm solutions, 50 μg mL^{-1} or 100 μg mL^{-1} dsDNA was incubated with 500 μM Pd(II)−Spd or Pd(II)−Spm, in pH 7.0, 0.1 M phosphate buffer, at room temperature, during 24 h.

Nondenaturing agarose (0.5%, ultrapure DNA grade from Sigma) gels were prepared in TAE buffer (10 mM Tris base, 4.4 mM acetic acid, and 0.5 mM EDTA, pH 8.0). Forty microliters of control dsDNA and DNA−Pd(II)−Spd and DNA−Pd(II)−Spm sample aliquots (with 0.25% bromophenol blue) were loaded into wells, and electrophoresis was carried out in TAE buffer for 90 min at 100 V. After this, 2% ethidium bromide (EtBr) stained DNA was visualized and photographed. Photographs were taken under UV (312 nm) transillumination to visualize DNA mobility.

Sample Preparation. The interaction of Spd, Spm, Pd(II)−Spd, and Pd(II)−Spm with dsDNA was studied on HOPG and GC electrodes by MAC mode AFM in air and voltammetric methods, using the procedures described below.

Procedure 1: DNA−Spd, DNA−Spm, DNA−Pd(II)−Spd, and DNA−Pd(II)−Spm Modified HOPG. For the preparation of control dsDNA modified HOPG were used solutions of 5 μg mL^{-1} or 10 μg mL^{-1} dsDNA in pH 7.0, 0.1 M phosphate buffer, stored at room temperature during 2, 12, or 24 h. For the preparation of DNA−Spd, DNA−Spm, DNA−Pd(II)−Spd, and DNA−Pd(II)−Spm modified HOPG, 5 μg mL^{-1} or 10 μg mL^{-1} dsDNA was incubated with either 10 μM or 50 μM Spd, Spm, Pd(II)−Spd, or Pd(II)−Spm, in pH 7.0, 0.1 M phosphate buffer, at room temperature, during 2, 12, and 24 h. Then, 200 μL samples of the desired solution were placed onto the freshly cleaved HOPG for 10 min. The excess of solution was removed with Millipore Milli-Q water, and the modified HOPG was dried in a sterile atmosphere.

Procedure 2: Control dsDNA, DNA−Spd, DNA−Spm, DNA−Pd(II)−Spd, and DNA−Pd(II)−Spm Modified GC Electrode. The control dsDNA, DNA−Spd, DNA−Spm, DNA−Pd(II)−Spd, and DNA−Pd(II)−Spm modified GC electrode were obtained by spontaneous adsorption, depositing a volume of 5 μL of the desired solution onto a clean GC surface for 10 min. After modification, the GC electrode was washed with Millipore Milli-Q water to ensure the removal of nonadsorbed molecules and was transferred to pH 4.5, 0.1 M acetate buffer.

RESULTS

The mechanism of interaction of Pd(II)−Spd and Pd(II)−Spm with dsDNA was investigated and characterized by AFM and voltammetry, based on different morphological and voltammetric modifications observed at the HOPG and GC electrodes. The results were compared with the interaction established in similar experimental conditions by their ligands Spd and Spm with dsDNA.

AFM Evaluation of the Pd(II)−Spd and Pd(II)−Spm Interaction with dsDNA. For a correct evaluation of the dsDNA conformational modifications after interaction with the Spd, Spm, Pd(II)−Spd, and Pd(II)−Spm molecules, in the AFM study, were used small concentrations of 5 μg mL^{-1} and 10 μg mL^{-1} dsDNA and 10 μM and 50 μM Spd, Spm, Pd(II)−Spd, and Pd(II)−Spm, prepared in pH 7.0, 0.1 M phosphate buffer. An atomically flat HOPG electrode was used as a substrate with less than 0.06 nm of root-mean-square (rms) roughness for a 1000 × 1000 nm^2 surface area. The GC electrode used for the voltammetric characterization was much rougher, with 2.10 nm rms roughness for the same surface area, therefore unsuitable for AFM surface characterization. Furthermore, the experiments using GC electrode and HOPG electrodes showed similar electrochemical behavior.

In order to determine the interaction of Spd, Spm, Pd(II)−Spd, and Pd(II)−Spm with dsDNA, the HOPG electrode was modified by DNA−Spd, DNA−Spm, DNA−Pd(II)−Spd, and DNA−Pd(II)−Spm films, obtained as described in Procedure 1 from the Experimental Section, by spontaneous adsorption during 10 min from incubated solutions of dsDNA with Spd, Spm, Pd(II)−Spd, or Pd(II)−Spm, during 2, 12, and 24 h. This procedure led to the coadsorption of DNA−drug, free dsDNA, and free drug molecules.[25]

Aiming at establishing the dsDNA control adsorption pattern, AFM was employed to study the spontaneous adsorption of dsDNA from solutions of 5 μg mL^{-1} and 10 μg mL^{-1} dsDNA, as described in Procedure 1. The AFM topographical images in air of the dsDNA film obtained from 5 μg mL^{-1} dsDNA showed coiled dsDNA molecules (not showed), while images from 10 μg mL^{-1} dsDNA showed a thin network (Figure 1A), both presenting heights of 1.4 ± 0.3 nm. After storing the dsDNA solutions for 24 h (Figure 1B), the HOPG surface coverage by dsDNA molecules and films decreased slightly, presenting a thickness of 1.5 ± 0.3 nm.

Interaction of Polyamines with dsDNA. The DNA process of adsorption on the HOPG surface, following the interaction with the biogenic polyamines Spd and Spm, is essential to explain the interaction of Pd(II)−Spd and Pd(II)−Spm with dsDNA. The dimensions of approximately 1.5 nm for the Spd and 2.0 nm for the Spm of the totally N-protonated all trans conformations, Scheme 1, are similar to the diameter of the B-form of the long calf-thymus DNA used in this study.

AFM images of the DNA−Spm modified HOPG obtained from an incubated solution of 10 μg mL^{-1} dsDNA with 50 μM Spm during 2 h showed the formation of a DNA−Spm network (Figure 1C), with the same morphological structure as the control dsDNA network films (Figure 1A) and an average height and standard deviation of 1.7 ± 0.3 nm. After 24 h incubation time, the height of the DNA−Spm layer decreased slightly to 1.4 ± 0.2 nm (Figure 1D).

AFM images of a DNA−Spd modified HOPG surface obtained from a solution of 10 μg mL^{-1} dsDNA with 50 μM Spd, incubated

(25) Corduneanu, O.; Chiorcea-Paquim, A.-M.; Fiuza, S. M.; Marques, M. P. M.; Oliveira-Brett, A. M. *Bioelectrochemistry* **2009**, DOI: 10.1016/j.bioelechem.2009.08.003.

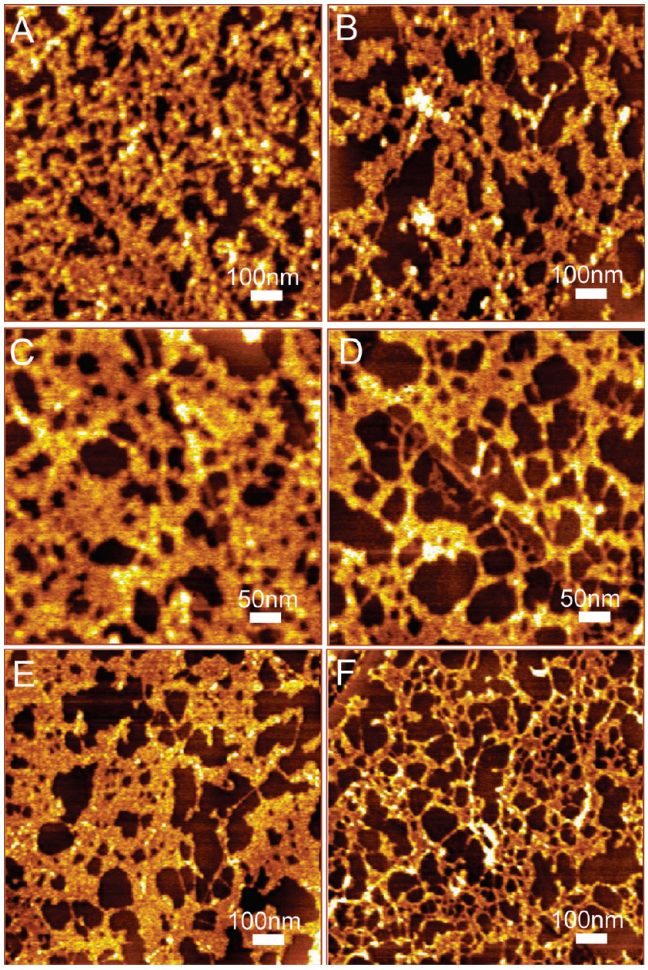

Figure 1. AFM images of (A, B) control dsDNA (C, D) DNA−Spm, and (E, F) DNA−Spd modified HOPG electrode obtained from solutions in pH 7.0, 0.1 M phosphate buffer of (A, B) 10 μg mL^{-1} dsDNA and (C−F) 10 μg mL^{-1} dsDNA incubated with (C, D) 50 μM Spm and (E, F) 50 μM Spd, after (A, C, E) 2 h and (B, D, F) 24 h.

during 2 h, showed a 1.6 ± 0.4 nm thick network (Figure 1E), while after a 24 h incubation the DNA−Spd layer became 1.4 ± 0.3 nm in height (Figure 1F).

Interaction of Pd(II)−Spd and Pd(II)−Spm with dsDNA. AFM images of a DNA−Pd(II)−Spm modified HOPG surface obtained from an incubated solution of 10 μg mL^{-1} dsDNA with 50 μM Pd(II)−Spm during 2 h also showed the formation of a network film (Figure 2A) with similar morphological characteristics as the control dsDNA (Figure 1A) and DNA−Spm (Figure 1C) networks and an average height and standard deviation of 1.9 ± 0.2 nm. The DNA−Pd(II)−Spm layer maintained the same surface coverage and pattern of adsorption after a 12 h incubation time and an average height of 2.0 ± 0.2 nm (Figure 2B), although high-resolution images showed the accumulation of small aggregates on the network arms, in general with heights between 3.0 and 4.0 nm (Figure 2C). The increase of the incubation time to 24 h led to an increase of the number and the height of the aggregates to 5.0−7.0 nm (Figure 2D).

A more complex situation was observed when dsDNA was incubated with Pd(II)−Spd complex. AFM images of the DNA−Pd(II)−Spd film formed with incubated solutions of 10 μg mL^{-1} dsDNA with 50 μM Pd(II)−Spd, during 2 h, showed the adsorption of a large number of molecular aggregates, with

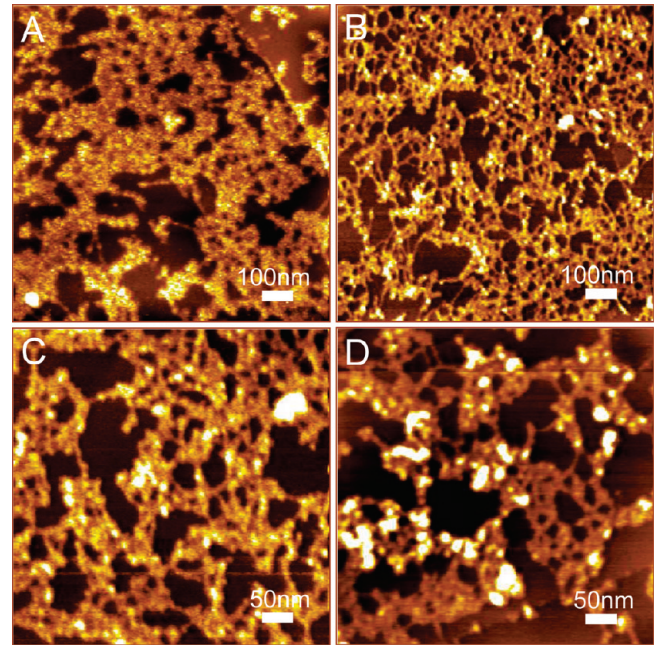

Figure 2. AFM images of DNA−Pd(II)−Spm modified HOPG electrode obtained from incubated solutions of 10 μg mL^{-1} dsDNA with 50 μM Pd(II)−Spm in pH 7.0, 0.1 M phosphate buffer, during (A) 2 h, (B, C) 12 h, and (D) 24 h.

heights between 12.0 and 20.0 nm, well distributed over the HOPG surface (Figure 3A). Increasing the incubation time to 12 h (Figure 3B), the aggregates became larger and higher, of 17.0−28.0 nm height. Higher magnification images showed the predisposition of the aggregates to adsorb near the HOPG step edges (Figure 3C), due to the formation of very compact DNA−Pd(II)−Spd structures, with the hydrophobic DNA bases hindered inside the condensed molecules. After a 24 h incubation, the size of the DNA−Pd(II)−Spd aggregates became larger, up to 34.0 nm height, with an even more reduced adsorption onto HOPG (Figure 3D).

In order to observe the aggregation process of the dsDNA by the Pd(II)−Spd complex, incubated solutions with smaller concentrations of 5 μg mL^{-1} dsDNA and 10 μM Pd(II)−Spd have also been investigated. The AFM images of the modified DNA−Pd(II)−Spd HOPG surface, formed by incubation during 2 h, show the formation of a thick and lumpy network film of 2.4 ± 0.6 nm height, with embedded aggregates up to 16 nm in height (Figure 3F). After a 24 h incubation time, only very large clusters where observed on the HOPG surface, due to a complete aggregation of the dsDNA by the Pd(II)−Spd (Figure 3F). The height of the DNA−Pd(II)−Spd aggregates was generally in the range of 15.0−20.0 nm.

Voltammetric Evaluation of the Pd(II)−Spd and Pd(II)−Spm Interaction with dsDNA. *Interaction of Polyamines with dsDNA.* For the voltammetric study of the dsDNA interaction with biogenic polyamines, solutions with a concentration of 100 μM Spd or Spm were prepared in pH 7.0, 0.1 M phosphate buffer. The interaction was followed by DP voltammetry, and the observed changes of the purine base oxidation peak currents, desoxyguanosine (dGuo), E_{pa} = +1.03 V, and desoxyadenosine (dAdo), E_{pa} = +1.30 V, were compared with the results obtained for a dsDNA control solution. The occurrence of the guanine and/or adenine oxidation product peaks, biomarkers

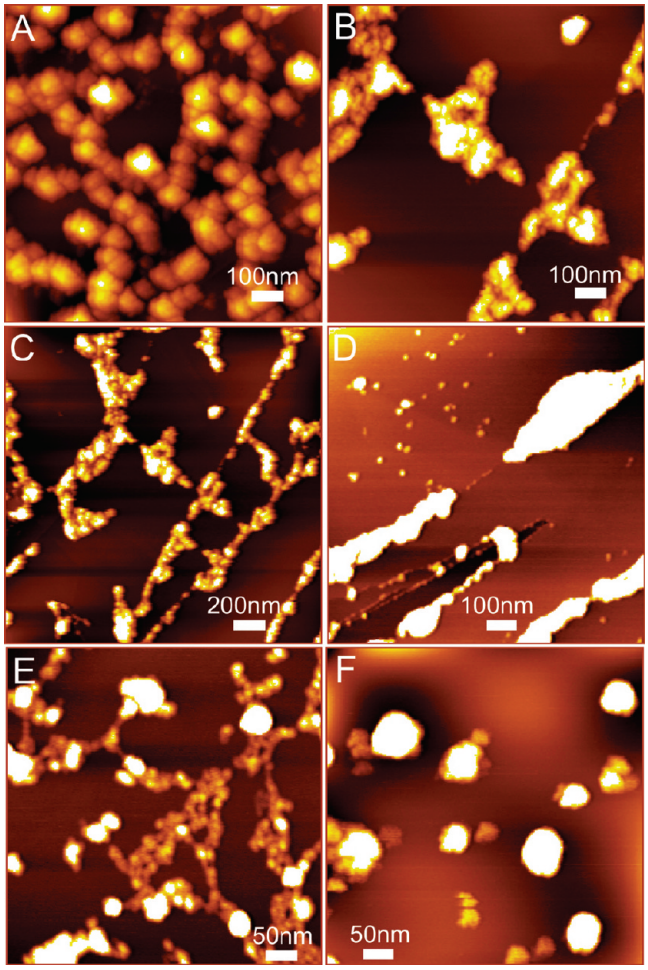

Figure 3. AFM images of DNA−Pd(II)−Spd modified HOPG electrode obtained from incubated solutions in pH 7.0, 0.1 M phosphate buffer of (A−D) 10 μg mL^{-1} dsDNA with 50 μM Pd(II)-Spd and (E, F) 5 μg mL^{-1} dsDNA with 10 μM Pd(II)-Spd, during (A, E) 2 h, (B, C) 12 h and (D, F) 24 h.

8-oxoguanine (8-oxoGua) and 2,8-dihydroxyadenine (2,8-DHA), $E_{pa} \sim +0.45$ V in pH 4.5, 0.1 M acetate buffer, is an indication of oxidative damage caused to DNA.[26,27]

Solutions of 50 μg mL^{-1} dsDNA were incubated with Spd or Spm in pH 7.0, 0.1 M phosphate buffer for different periods of time. A control solution of dsDNA was also prepared in pH 7.0, 0.1 M phosphate buffer and analyzed after the same periods of time as the DNA−Spd/Spm incubated solutions. The interaction was assessed by DP voltammetry in supporting electrolyte pH 4.5 with the DNA−Spd/Spm GC electrode modified as described in Procedure 2.

The DP voltammograms recorded for the solution of dsDNA incubated with 100 μM Spm for 2 and 24 h are presented in Figure 4A. The results showed a decrease of the dGuo and dAdo oxidation peaks after 2 h of incubation, compared with the peaks for the control dsDNA. After 24 h of incubation, the voltammograms showed a significant decrease of the DNA oxidation peaks, but no other peaks related to oxidation of 8-oxoGua or 2,8-DHA were detected.

(26) Oliveira-Brett, A. M.; Piedade, J. A. P.; Serrano, S. H. P. *Electroanalysis* **2000**, *12*, 969–973.
(27) Diculescu, V. C.; Piedade, J. A. P.; Oliveira-Brett, A. M. *Bioelectrochemistry* **2007**, *70*, 141–146.

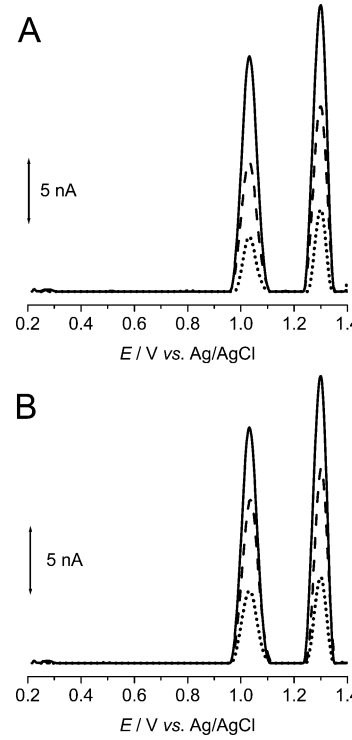

Figure 4. DP voltammograms in supporting electrolyte pH 4.5 of (—) control dsDNA and after (– – –) 2 h and (•••) 24 h of incubation with (A) 100 μM Spm and (B) 100 μM Spd.

For the solution of dsDNA incubated with 100 μM Spd (Figure 4B), the voltammograms recorded in supporting electrolyte at pH 4.5 showed similar results to those obtained for the incubation with Spm, i.e., a decrease in dGuo and dAdo oxidation peaks with increasing incubation time. However, it was observed that the peak currents decrease in the case of Spm is slightly higher, probably due to the existence of an additional positive charge that provides more sites available for binding to DNA.

Interaction of Pd(II)−Spd and Pd(II)−Spm with dsDNA. For the voltammetric evaluation of the interaction between dsDNA and the Pd(II) complexes, solutions of 100 μM Pd(II)−Spd or Pd(II)−Spm in 0.1 M phosphate buffer, pH 7.0, were used. This concentration was reported in a previous study where analogue Pt complexes were used in human cancer cell lines.[7] The control dsDNA solution of 50 μg mL^{-1} was also prepared in phosphate buffer, pH 7.0, and analyzed after the same periods of time as for the study of DNA interaction with Pd(II)−Spd and Pd(II)−Spm.

The first approach was to investigate the effect of the interaction of these Pd(II) complexes in short duration incubations. The surface of the GC electrode was modified with a layer of 50 μg mL^{-1} dsDNA as described in Procedure 2. The dsDNA modified electrode was immersed in the 100 μM solution of either Pd(II)−Spd or Pd(II)−Spm and incubated for 5, 10, or 30 min. After the incubation, the excess of solution was removed with Milli Q water, and the electrode was transferred to pH 4.5, 0.1 M acetate buffer.

The interaction between the Pd(II)−Spm complex and dsDNA was studied after a 10 min incubation in 100 μM Pd(II)−Spm. The voltammograms recorded showed a decrease of the dGuo and dAdo oxidation peaks (Figure 5A), noticeable in the case of the guanine residues when compared with the control dsDNA

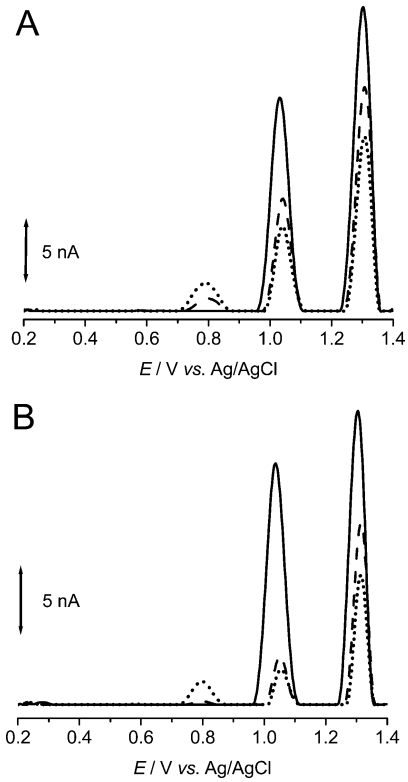

Figure 5. DP voltammograms in supporting electrolyte pH 4.5 of (—) control dsDNA and after (A) (– – –) 10 and (•••) 30 min incubation with 100 μM Pd(II)−Spm and (B) (– – –) 5 and (•••) 10 min incubation with 100 μM Pd(II)−Spd.

oxidation peaks. In addition to this effect, another oxidation peak at +0.80 V was detected. For this reason, the incubation time with the Pd(II)−Spm complex was increased to 30 min, and the occurrence of the oxidation peak at +0.80 V, corresponding to oxidation of the free guanine base,[28] was confirmed. However, no peaks related to the presence of oxidative damage biomarkers, 8-oxoGua or 2,8-DHA, were detected.

The interaction between Pd(II)−Spd and dsDNA showed a similar effect, i.e., a decrease of the DNA peaks after the interaction (Figure 5B) but with a significant current decrease in relation to the currents recorded for the interaction with the Pd(II)−Spm complex. It was observed that the dGuo and dAdo peaks continued to decrease with increasing incubation time, while the peak current of free guanine increased.

In another experiment, the GC electrode was modified with a layer of DNA−Pd(II)−Spd/Pd(II)−Spm from a solution of dsDNA incubated for 12 h with 100 μM Pd(II)−Spd or Pd(II)−Spm complex (Figure 6). The voltammograms recorded in supporting electrolyte, pH 4.5, confirmed the results observed for the short time incubations. A considerable decrease of the dGuo and dAdo oxidation peaks after 12 h of incubation was observed for the dsDNA solution incubated with the Pd(II)−Spm complex, and the absence of peaks was observed in the case of dsDNA incubated with the Pd(II)−Spd. The voltammograms showed also that the oxidation peak of free guanine occurs for the incubation with the Pd(II)−Spm complex; while for the incubation with Pd(II)−Spd,

(28) Oliveira-Brett, A. M.; Piedade, J. A. P.; Silva, L. A.; Diculescu, V. C. *Anal. Biochem.* **2004**, *332*, 321–329.

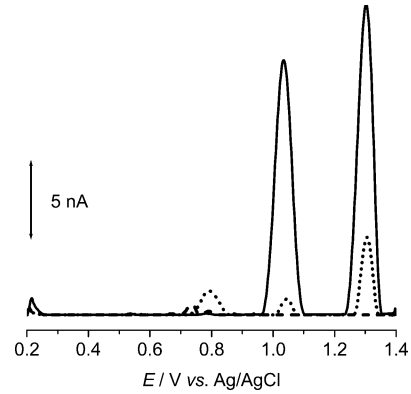

Figure 6. DP voltammograms in supporting electrolyte pH 4.5 of (—) control dsDNA after 12 h from preparation, and DNA incubated for 12 h with (•••) 100 μM Pd(II)−Spm and (– – –) 100 μM Pd(II)−Spd.

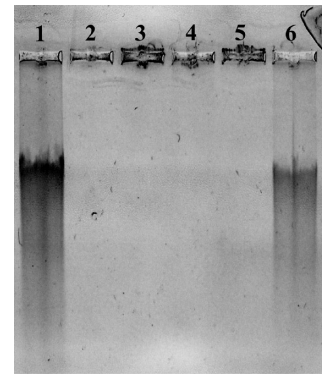

Figure 7. Nondenaturing agarose (0.5%) gel electrophoresis showing the migration profiles: lane 1 (100 μg mL^{-1} control dsDNA), lane 2 (100 μg mL^{-1} dsDNA with 500 μM Pd(II)−Spd), lane 3 (100 μg mL^{-1} dsDNA with 500 μM Pd(II)−Spm), lane 4 (50 μg mL^{-1} dsDNA with 500 μM Pd(II)−Spd), lane 5 (50 μg mL^{-1} dsDNA with 500 μM Pd(II)−Spm), and lane 6 (50 μg mL^{-1} control dsDNA).

the guanine oxidation peak is very small. However, no oxidative damage to DNA was detected.

Electrophoresis Evaluation of the Pd(II)−Spd and Pd(II)−Spm Interaction with dsDNA. To evaluate the morphological modifications obtained before and after the dsDNA interaction with both the complexes, Pd(II)−Spd and Pd(II)−Spm, 0.5% nondenaturing agarose gel electrophoresis was performed as described in the Experimental Section. The migration profile of the control dsDNA samples was compared with that of DNA−Pd(II)−Spd and DNA−Pd(II)−Spm after incubation of 50 μg mL^{-1} or 100 μg mL^{-1} dsDNA with 500 μM Pd(II)−Spd and Pd(II)−Spm, in pH 7.0, 0.1 M phosphate buffer, during 24 h. To visualize the dsDNA, DNA−Pd(II)−Spd and DNA−Pd(II)−Spm mobility, the EtBr binding assay for DNA, that forms a strong fluorescent complex with dsDNA, was used.

Figure 7 shows the obtained electrophoretic migration profiles: lane 1 (100 μg mL^{-1} control dsDNA), lane 2 (100 μg mL^{-1} dsDNA with 500 μM Pd(II)−Spd), lane 3 (100 μg mL^{-1} dsDNA with 500 μM Pd(II)−Spm), lane 4 (50 μg mL^{-1} dsDNA with 500 μM Pd(II)−Spd), lane 5 (50 μg mL^{-1} dsDNA with 500 μM Pd(II)−Spm), and lane 6 (50 μg mL^{-1} control dsDNA).

The bands present in the control dsDNA samples (lanes 1 and 6) are due to different-sized long fragments present in the calf-

thymus dsDNA, and the intensity of the bands diminished, as expected, with decreasing concentration of dsDNA. In all DNA samples incubated with Pd(II)−Spd and Pd(II)−Spm, the EtBr fluorescence disappeared when compared with the control ds-DNA, which is an indication of the occurrence of perturbations in the DNA double-stranded structure, which made impossible the binding of the EtBr marker to the very condensed aggregated DNA−Pd(II)−Spd and DNA−Pd(II)−Spm samples.

DISCUSSION

The AFM and voltammetric results obtained for the dsDNA interaction with the complexes Pd(II)−Spd (Figures 3, 5B, and 6) and Pd(II)−Spm (Figures 2, 5A, and 6) have been evaluated and compared with the control dsDNA modified HOPG (Figure 1A,B) or GC (Figures 5 and 6(−)) electrodes and with the results obtained for the dsDNA interaction with Spd (Figures 1E,F and 4B) and Spm (Figures 1C,D and 4A). The polyamine concentrations used for the study of the DNA−Spd/Spm interactions and the ionic strength of the interaction medium are very low in comparison with the conditions reported in the literature for DNA precipitation.[20] These experimental conditions were chosen to illustrate the relevant information for the interaction of dsDNA with the Pd(II) complexes, in which these polyamines were used as ligands.

The AFM and voltammetric results obtained after the incubation of dsDNA with Spd and Spm showed that an interaction occurs even for low concentrations of 50−100 μM, compared to the concentrations of milimolar level present in cells or used for DNA precipitation and purification. AFM images showed a DNA−Spd/Spm pattern of adsorption similar with the one of control dsDNA but with a slightly increased thickness after short incubation times (Figure 1C−F). In addition, the DP voltammetry shows a decrease of both dGuo and dAdo oxidation peaks when compared with the control dsDNA, consistent with their biological activity as compaction agents,[21] and as expected, the interaction of these polyamines with DNA caused no oxidative damage (Figure 4). The results presently obtained indicate that the structural characteristics of these polyamines may be relevant for the development of new cytotoxic agents, in view of increasing the selectivity of the drugs and allowing an efficient interaction with DNA for the treatment of neoplastic disorders.

Previous AFM and voltammetric results[29] demonstrated that Pd^{2+} interacts specifically with dsDNA, due to a high tendency of forming covalent bonds with nitrogenous bases, and induces structural changes in B-DNA. A reorganization of the DNA self-assembled network on the surface of the HOPG electrode was observed after the interaction of 10 μg mL^{-1} dsDNA with high concentrations of 100 μM Pd^{2+}, leading to the formation of thicker aggregates of the Pd−DNA complex caused by DNA condensation, when compared with the control dsDNA in the same experimental conditions.[29]

However, no free Pd(II) ion is expected to be present in the solutions of Pd(II)−Spd and Pd(II)−Spm complexes, since the synthesized chelates with polyamine ligands were shown to be stable, by spectroscopic detection as a function of time under physiological conditions.[6−9] In fact, the occurrence of significant concentrations of this free metal ion would have serious consequences regarding cell growth and differentiation, due to its high affinity for thioenzymes and other sulfur-containing essential biomolecules (e.g., glutathione). Moreover, the studies carried out up to now on the antiproliferative and cytotoxic properties of this kind of polynuclear polyamine Pd(II) and Pt(II) complexes show only the effect of the chelates.[6−9]

The DNA aggregation observed by AFM after interaction with both the Pd(II)−Spd and Pd(II)−Spm complexes (Figures 3 and 2, respectively) and the voltammetric results (Figures 5 and 6) suggest that the Pd(II) complexes induce more severe morphological changes in the dsDNA structure, when compared with the modifications induced by both the free ligands, Spd (Figures 1E,F and 4B) and Spm (Figures 1C,D and 4A), and by Pd^{2+}.[29]

The thickness of the DNA−Pd(II)−Spm lattice (Figure 2) presents values of 1.9−2.0 nm in height and up to 7.0 nm in height for embedded aggregates, higher than the thickness of the control dsDNA of 1.4−1.5 nm in height, meaning that several DNA layers are involved in an aggregation process. The interaction with DNA−Pd(II)−Spd was revealed to be even stronger, leading to the formation of very compact DNA−Pd(II)−Spd structures, up to 34.0 nm in height, with reduced adsorption onto HOPG (Figure 3).

The interaction of both Pd(II) complexes with the dsDNA was also detected voltammetrically, through the decrease observed in the dGua and dAdo oxidation peaks (Figures 5 and 6). This decrease of the oxidation peaks is a consequence of the reduced contact of the DNA bases with the GC electrode surface, as a result of the DNA conformational changes and aggregation, higher in the case of the Pd(II)−Spd complex (Figures 3, 5, and 6).

The electrophoretic experiments confirm the effects caused by Pd(II)−Spd or Pd(II)−Spm on dsDNA (Figure 7). The disappearance of the fluorescence observed for both DNA−Pd(II)−Spd (lanes 2 and 4) and DNA−Pd(II)−Spm (lanes 3 and 5), when compared with control dsDNA (lanes 1 and 6), shows that the EtBr marker is excluded from intercalating in the dsDNA binding sites due to the strong condensation of the dsDNA caused by the Pd complexes. In addition, brighter wells were observed for DNA−Pd(II)−Spm (lanes 3 and 5), suggesting that some EtBr molecules are intercalated in unmodified dsDNA segments due to less significant DNA conformational changes and aggregation for DNA−Pd(II)−Spm when compared with DNA−Pd(II)−Spd. Furthermore, the DNA−Pd(II)−Spm/Pd(II)−Spd aggregates presented a much lower electrophoretic mobility in the gel, when compared with the control dsDNA. Consequently, it can be concluded that a DNA conformational transition occurred during incubation with both Pd(II)−Spd and Pd(II)−Spm, which led to condensation and modification of the DNA secondary structure.

AFM, voltammetric, and electrophoresis results clearly showed that the Pd(II)−Spd complex presents a stronger interaction with dsDNA. In addition, the voltammetric results indicate that the interaction of the Pd(II) complexes with the dsDNA may follow the same mechanism, although with a slower kinetics for the Pd(II)−Spm complex. This effect is explained by the structural differences of these two complexes. The Pd(II)−Spd complex is not only a trinuclear cisplatin-like chelate[8] with an additional bifunctional alkylating center than the Pd(II)−Spm complex but also it displays a more elongated shape due to the presence of

(29) Chiorcea-Paquim, A.-M.; Corduneanu, O.; Oliveira, S. C. B.; Diculescu, V. C.; Oliveira-Brett, A. M. *Electrochim. Acta* **2009**, *54*, 1978–1985.

two Spd units, which may favor the interaction with dsDNA. The Pd(II)−Spm complex, in turn, comprises two identical units, each with a bifunctional Pd center linked to nitrogen atoms of only one Spm molecule. For both complexes, all nitrogen atoms are coordinated to Pd centers,[7] which affects the mobility and the ability of the ligands to establish electrostatic interactions with negatively charged phosphate groups of the DNA double helix. However, these complexes, as well as their Pt analogues, were found to be effective against human cancer cell lines;[7] their mechanism of interaction is probably related to the presence of multiple alkylation centers. The Pd(II)−Spd complex showed even a greater activity in human cancer cell lines than its Pt analogue.[8]

Structural and kinetic techniques demonstrated that the Pd(II) complexes, as well as the less reactive Pt(II) complexes, present a strong preference for the N7 site of the guanine and adenine residues, leading to the formation of adducts, by intra- and interstrand cross-links.[30−33] Due to the existence of multiple centers of alkylation, with six possible coordination sites with the DNA double helix for the Pd(II)−Spd complex and four for Pd(II)−Spm, these complexes have a high affinity toward the formation of covalent bonds with the nitrogenous bases, similar to the antitumor drug cisplatin and a number of other Pt(II) and Pd(II) complexes. This selective binding observed for the Pd(II) polyamine complexes results in a distortion and local denaturation of the DNA double helix, due to the disruption of the base pairing and base stacking, and in the release of some guanine bases, which were directly detected by voltammetry (Figure 5). The formation of adducts and aggregates due to palladium intra- and interstrand cross-links,[30−33] was also observed by AFM and voltammetry, being particularly clear in the case of the Pd(II)−Spd complex (Figures 2, 3, and 6). The observed DNA morphological modification and aggregation increased with increasing concentration of complexes and incubation time.

CONCLUSIONS

The interaction with dsDNA of two polynuclear Pd(II) chelates with the biogenic polyamines Spd and Spm was studied at room temperature, using AFM, voltammetry, and gel electrophoresis. After the interaction with Pd(II)−Spd and Pd(II)−Spm, a reorganization of the DNA self-assembled network on the surface of the HOPG electrode and a decrease in dGua and dAdo oxidation peaks is observed. These results are consistent with the model in the literature describing the mechanism of interaction of Pd(II) and Pt(II) complexes with dsDNA that leads to the formation of DNA adducts and/or aggregates. The Pd(II)−Spd complex presents a stronger interaction with dsDNA, owing to its molecular structure comprising three Pd(II) centers and two Spd molecules, with six possible coordination sites to dsDNA, as compared to Pd(II)−Spm that contains only two Pd(II) ions and one Spm ligand, yielding only four possible coordination sites. Furthermore, the voltammetric results showed that the interaction with either of the Pd(II) polyamine complexes caused no oxidative damage to dsDNA.

Due to their polycationic chains, the polyamines Spd and Spm interact specifically with the negatively charged phosphate groups of the DNA double helix by electrostatic forces, thus stabilizing its structure. The voltammetric results show that the interaction is observed even at a low concentration of polyamines but causing no oxidative damage to DNA.

The results obtained along the present study suggest a strong correlation between the structure of these Pd(II) polyamine complexes and their interaction with DNA, which is critical for the development of new effective and selective cytotoxic drugs. Additionally, the voltammetric and AFM techniques represent fast and easy methods of testing the selectivity and effectiveness of the interaction of new drugs with dsDNA.

(30) Rau, T.; van Eldik, R. In *Metal ions in biological systems*; Sigel, A., Sigel, H., Eds.; Marcel Dekker, Inc.: New York, 1996; Vol. 32, pp 339−378.

(31) Probing nucleic acids by metal ion complexes of small molecules. In *Metal ions in biological systems*; Sigel, A., Sigel, H., Eds.; Marcel Dekker, Inc.: New York, 1996; Vol. 33.

(32) Natile, G.; Coluccia, M. In *Metal ions in biological systems*; Sigel, A., Sigel, H., Eds.; Marcel Dekker, Inc.: New York, 2004; Vol. 32, pp 209−250.

(33) Chiorcea-Paquim, A.-M.; Corduneanu, O.; Oliveira, S. C. B.; Diculescu, V. C.; Oliveira-Brett, A. M. *Electrochim. Acta* **2009**, *54*, 1978–1985.

ACKNOWLEDGMENT

Financial support from Fundação para a Ciência e Tecnologia (FCT), Ph.D. Grants SFRH/BD/18914/2004 (O.C.) and SFRH/BD/17493/2004 (S.M.F.), Post-Doctoral Grant SFRH/BPD/36110/2007 (V.C. Diculescu), projects PTDC/QUI/65255/2006 and PTDC/QUI/098562/2008, POCI 2010 (cofinanced by the European Community Fund FEDER), and CEMUC-R (Research Unit 285) are gratefully acknowledged.

Received for review September 22, 2009. Accepted January 11, 2010.

AC902127D